Hindawi Publishing Corporation
Mathematical Problems in Engineering
Volume 2014, Article ID 914616, 10 pages
http://dx.doi.org/10.1155/2014/914616

Research Article

Robust Sampled-Data H_∞ Control for Vibration Mitigation of Offshore Platforms with Missing Measurements

Mingjie Cai,[1] Zhengrong Xiang,[1] and Hamid Reza Karimi[2]

[1] *School of Automation, Nanjing University of Science and Technology, Nanjing 210094, China*
[2] *Department of Engineering, Faculty of Engineering and Science, University of Agder, 4898 Grimstad, Norway*

Correspondence should be addressed to Zhengrong Xiang; xiangzr@mail.njust.edu.cn

Received 27 December 2013; Accepted 27 January 2014; Published 4 March 2014

Academic Editor: Weichao Sun

Copyright © 2014 Mingjie Cai et al. This is an open access article distributed under the Creative Commons Attribution License, which permits unrestricted use, distribution, and reproduction in any medium, provided the original work is properly cited.

This paper presents a robust sampled-data H_∞ control for vibration attenuation of offshore platforms with missing measurements subject to external wave force. It is well known that the phenomena of missing measurements are unavoidable due to various reasons, such as sensor aging and sensor temporal failure, which may degrade the control system performance or even cause instability. For active vibration control of offshore platforms with sampling measurements, to deal with the missing measurements, a robust sampled-data H_∞ control method is proposed in this paper. The robust sampled-data H_∞ state feedback controller is obtained in terms of the solvability of certain linear matrix inequalities (LMIs). Finally, simulations on an offshore platform are exploited to demonstrate the effectiveness of the proposed method. The simulation results show that the designed robust sampled-data H_∞ control scheme is effective to attenuate the external wave force in the presence of missing measurements.

1. Introduction

In the modern world, the offshore platforms, especially the oil and gas production platforms, play a more and more important role. The offshore platforms generally undergo various disturbances coming from the hostile environment that they are located in, such as wave, wind, ice, and earthquake, and the self-excited nonlinear hydrodynamic force [1, 2]. These external loads inevitably induce large continuous vibrations which make the offshore platform deformation, fatigue damage, and even unsafety. To prevent fatigue damage and ensure safety and production efficiency, the vibrations of the offshore platforms should be limited.

Up to now, a large number of researches have been made to improve the control performance of the system via active control scheme. For example, for offshore steel jacket platforms with an active tuned mass damper (TMD) mechanism, the multiloop feedback design method [1], the nonlinear control scheme, and the robust state feedback control scheme [2] have been developed to reduce the internal oscillation amplitudes of the offshore platforms. By using an active mass damper (AMD), some optimal control based schemes have been applied to improve the performance of the jacket platforms [3–6]. Recently, the dynamic output feedback control scheme [7] and the integral sliding mode control method [8, 9] have been presented to improve the performance of the offshore platforms. More recently, a delay-dependent state feedback controller has been developed to stabilize the offshore platforms subject to self-excited hydrodynamic force and actuator time-delays [10]. In [11], by artificially introducing a proper time-delay into control channel, a delayed H_∞ controller is designed to attenuate the wave-induced vibration of the offshore platform and thereby improve the control performance of the system. It is indicated that the aforementioned active control schemes are effective ways to deal with the vibration problem of offshore platforms subject to nonlinear wave force.

It is well known that computers are usually used as digital controllers to control continuous-time systems in modern control systems [12] with the rapid progress of computer and digital technologies. With recent focus on wireless monitoring and control of offshore platforms [13–18] based on networked control technique [19], studying sampled-data control problem for offshore platforms is becoming significant, and the vibration control methods adopted in [1–11] are no longer applicable to offshore platforms with sampling measurements. On the other hand, because of various reasons, such as sensor aging and sensor temporal failure, the phenomena of missing measurements are unavoidable, which may degrade the control system performance or even cause instability [20–26]. Thus, it is necessary to consider the missing measurements encountered in practical issues for vibration control. However, to the best of our knowledge, no results have been made on sampled-data H_∞ control for vibration attenuation of offshore platforms in presence of missing measurements, which motivates our work in this paper.

This paper is concerned with the robust sampled-data H_∞ controller design for vibration attenuation of offshore platforms subject to missing measurements and external wave force. The issue of vibration attenuation is transformed into an H_∞ disturbance attenuation problem of the system. A Lyapunov functional approach is used to solve the H_∞ disturbance attenuation problem, and the controller design is formulated in terms of linear matrix inequalities (LMIs). To validate the effectiveness of the proposed approach, the designed controllers are applied to reduce the vibration of an offshore platform. Simulation results show good vibration attenuation performance in spite of involving missing measurements.

The rest of this paper is organized as follows. In Section 2, the description of an offshore platform with an AMD mechanism is given first. Then, the formulation of robust sampled-data H_∞ control problem with missing measurements is presented. In Section 3, the robust sampled-data H_∞ controller design problem involving missing measurements is solved. An illustrative example is given in Section 4, and we conclude the paper in Section 5.

Notation. The notation used in the paper is fairly standard. The superscript "T" stands for matrix transposition; R denotes the space of real numbers; R^n denotes the n-dimensional Euclidean space; the notation $P > 0$ (≥ 0) means that the matrix P is real symmetric and positive definite (semidefinite); I and 0 represent the identity matrix and zero matrix of appropriate dimensions, respectively; $\mathscr{L}$ is the infinitesimal operator; and diag$\{\cdot\}$ stands for a block-diagonal matrix. In addition, $E\{x\}$ means expectation of the stochastic variable x. The space of square-integrable vector functions over $[0,\infty)$ is denoted by $L_2[0,\infty)$ and for $f(t) \in L_2[0,\infty)$, its norm is given by $\|f(t)\|_2 = \sqrt{\int_{t=0}^{\infty} f^T(t) f(t)\, dt}$. For simplicity, the symmetric term in a symmetric matrix is denoted by "$*$."

2. Problem Formulation

In this section, a dynamic model of an idealized two-degree-of-freedom system with an AMD mechanism will be presented and the active vibration attenuation problem for the system with sampling measurements will be formulated by applying a state feedback control scheme.

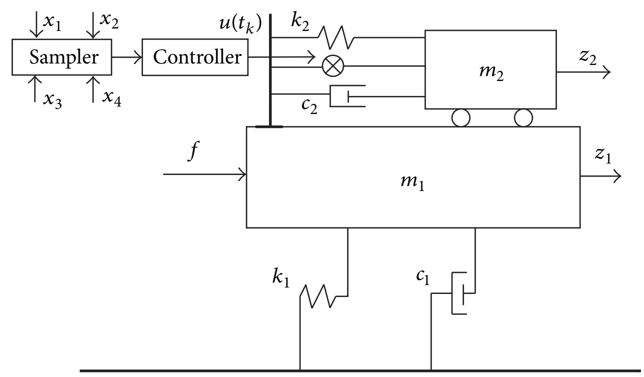

Figure 1: Schematic diagram of offshore platform with AMD.

Consider an offshore platform shown in Figure 1 [11]; the dynamic equations of the offshore platform can be described as

$$\begin{aligned} m_1 \ddot{z}_1(t) = & -\left(m_1\omega_1^2 + m_2\omega_2^2\right) z_1(t) + m_2\omega_2^2 z_2(t) + f(t) \\ & - u(t) - 2\left(m_1\xi_1\omega_1 + m_2\xi_2\omega_2\right)\dot{z}_1(t) \\ & + 2m_2\xi_2\omega_2\dot{z}_2(t), \\ m_2\ddot{z}_2(t) = & \, m_2\omega_2^2 z_1(t) + 2m_2\xi_2\omega_2\dot{z}_1(t) - m_2\omega_2^2 z_2(t) + u(t) \\ & - 2m_2\xi_2\omega_2\dot{z}_2(t), \end{aligned} \tag{1}$$

where $z_1(t)$ and $z_2(t)$ are displacements of the deck motion of the offshore platform and the AMD, respectively; m_1, ω_1, and ξ_1 are the modal mass, natural frequency, and damping ratio of the offshore platform, respectively; m_2, ω_2, and ξ_2 are the mass, natural frequency, and damping ratio of the AMD, respectively; $u(t)$ is the active control of the system; $f(t)$ is the external wave force acting on the offshore platform and can be numerically calculated by referring to [6].

Define the following state variables:

$$\begin{aligned} x_1(t) &= z_1(t), & x_2(t) &= z_2(t), \\ x_3(t) &= \dot{z}_1(t), & x_4(t) &= \dot{z}_2(t), \end{aligned} \tag{2}$$

and let

$$x(t) = \left[x_1(t) \;\; x_2(t) \;\; x_3(t) \;\; x_4(t)\right]^T. \tag{3}$$

Then, the dynamic model of the offshore platform (1) can be written as

$$\dot{x}(t) = Ax(t) + Bu(t) + Df(t), \quad x(0) = x_0, \tag{4}$$

where

$$A = \begin{bmatrix} 0 & 0 & 1 & 0 \\ 0 & 0 & 0 & 1 \\ -\left(\omega_1^2 + \omega_2^2 \frac{m_2}{m_1}\right) & \omega_2^2 \frac{m_2}{m_1} & -2\left(\xi_1 \omega_1 + \xi_2 \omega_2 \frac{m_2}{m_1}\right) & 2\xi_2 \omega_2 \frac{m_2}{m_1} \\ \omega_2^2 & -\omega_2^2 & 2\xi_2 \omega_2 & -2\xi_2 \omega_2 \end{bmatrix},$$

$$B = \begin{bmatrix} 0 & 0 & -\frac{1}{m_1} & \frac{1}{m_2} \end{bmatrix}^T, \qquad D = \begin{bmatrix} 0 & 0 & \frac{1}{m_1} & 0 \end{bmatrix}^T. \tag{5}$$

To guarantee the performance index from the wave force $f(t)$ to the control output $\xi(t)$ to be realized with the specified requirement, the displacement response $x_1(t)$ and the velocity response $x_3(t)$ of the offshore platform are chosen as the control output. In this situation, the control output equation is given as

$$\xi(t) = C_1 x(t), \tag{6}$$

where

$$C_1 = \begin{bmatrix} 1 & 0 & 0 & 0 \\ 0 & 0 & 1 & 0 \end{bmatrix}. \tag{7}$$

In practice, for offshore platform system, only sampled measurements of state variables are available at discrete instants of time. Without loss of generality, it is assumed that the state variables of the active vibration system are measured at time instants $0 = t_0 < t_1 < \cdots < t_k < t_{k+1} \ldots$; that is, only $x(t_k)$ is available for interval $[t_k, t_{k+1})$, where $t_{k+1} - t_k \le h$ and h is the maximum sampling interval. We are interested in designing a state feedback controller, which may contain missing measurements described by

$$u(t) = u(t_k) = r(t_k) K x(t_k), \quad t_k \le t < t_{k+1}, \tag{8}$$

where K is the controller gain matrix to be designed and $r(t_k) \in R$ is the stochastic variable having the probabilistic density function $q(r(t_k))$ on the interval $[0, 1]$ with mathematical expectation b and variance σ^2; that is,

$$\begin{gathered} E\{r(t_k)\} = b, \\ E\{r^2(t_k)\} = [E\{r(t_k)\}]^2 + \sigma^2 = b^2 + \sigma^2, \end{gathered} \tag{9}$$

where $b \in R$ and $\sigma \in R$ are known positive scalars.

Remark 1. In real systems, due to various reasons, such as sensor aging and sensor temporal failure, the measurements missing at one moment might be partial and therefore the missing probability cannot be simply described by 0 or 1 [24]. It is easy to see that the widely used Bernoulli distribution is included here as a special case.

According to (4) and (8), the closed-loop system is given by

$$\begin{gathered} \dot{x}(t) = Ax(t) + r(t_k) BKx(t_k) + Df(t), \\ \xi(t) = C_1 x(t), \quad t_k \le t < t_{k+1}. \end{gathered} \tag{10}$$

It should be noticed that the closed-loop system (10) is actually a stochastic system, since it contains the stochastic quantity $r(t_k)$. Therefore, in the sequel, we will use the notion of stochastic stability in the mean-square sense.

Here, the issue of vibration attenuation for the offshore platform can be transformed into an H_∞ disturbance attenuation problem of system (10). The objective is to determine the controller (8) such that

(1) the closed-loop system (10) with $f(t) = 0$ is asymptotically mean-square stable;

(2) under zero initial condition, the H_∞ performance

$$E\{\|\xi(t)\|_2\} \le \gamma E\{\|f(t)\|_2\}, \tag{11}$$

of the closed-loop system (10) is guaranteed for nonzero $f(t) \in L_2[0, \infty)$ and a prescribed $\gamma > 0$.

To obtain the main results, the following lemma is needed.

Lemma 2 (Schur complement [24]). *Given constant matrices S_1, S_2, and S_3, where $S_1 = S_1^T$ and $0 < S_2 = S_2^T$, then $S_1 + S_3^T S_2^{-1} S_3 < 0$ if and only if*

$$\begin{bmatrix} S_1 & S_3^T \\ S_3 & -S_2 \end{bmatrix} < 0 \quad or \quad \begin{bmatrix} -S_2 & S_3 \\ S_3^T & S_1 \end{bmatrix} < 0. \tag{12}$$

3. Main Results

In this section, we will solve the problem of robust sampled-data H_∞ controller design for systems (4) and (6) with missing measurements by the recently developed input delay approach [27–29]. The key idea behind this approach is that we represent the sampling instant t_k as

$$t_k = t - (t - t_k) = t - d(t), \tag{13}$$

where $d(t) = t - t_k$. Then, from (8) and (13), we obtain

$$\begin{aligned} u(t) &= u(t_k) = u(t - d(t)) \\ &= r(t - d(t)) Kx(t - d(t)), \quad t_k \le t < t_{k+1}, \end{aligned} \tag{14}$$

where $u(t_k)$ is a discrete-time control signal and the time-varying delay $d(t)$ is piece-wise linear and satisfies $d(t) = t - t_k \le h$ and $\dot{d}(t) = 1$ for $t \ne t_k$. By using the input delay approach, the closed-loop system (10) can be transformed into a time-delay system as follows:

$$\begin{aligned} \dot{x}(t) &= Ax(t) + r(t - d(t)) BKx(t - d(t)) + Df(t), \\ \xi(t) &= C_1 x(t). \end{aligned} \tag{15}$$

In the following, we will determine the controller gain matrix K such that system (15) is asymptotically mean-square stable and satisfies the H_∞ disturbance attenuation in (11).

Remark 3. Recently, the vibration control problem for offshore platforms with constant input delay has been addressed in [10, 11]. It is worth pointing out that the transformed system in our problem contains nondifferentiable time-varying delay in the states, which hinders the results in [10, 11] to be directly applied to the problem considered here.

3.1. H_∞ Performance Analysis. The following theorem provides a sufficient condition for system (15) to be asymptotically mean-square stable and satisfy the H_∞ disturbance attenuation in (11).

Theorem 4. *Given scalars $h > 0$, $b > 0$, $\sigma > 0$ and controller gain matrix K, the closed-loop system (15) with $f(t) = 0$ is asymptotically mean-square stable and the H_∞ disturbance attenuation in (11) is satisfied for the wave force $f(t) \in L_2[0,\infty)$ and a prescribed $\gamma > 0$, if there exist matrices $P > 0$, $Q > 0$, $S_{11} > 0$, S_{12}, S_{13}, $S_{22} > 0$, and S_{23} with appropriate dimensions such that the following LMIs hold:*

$$S = \begin{bmatrix} S_{11} & S_{12} & S_{13} \\ * & S_{22} & S_{23} \\ * & * & Q \end{bmatrix} \geq 0, \quad (16)$$

$$\begin{bmatrix} \Psi_{11} & \Psi_{12} & PD & \sqrt{h}A^TQ & 0 & C_1^T \\ * & \Psi_{22} & 0 & \sqrt{h}bK^TB^TQ & \sqrt{h}\sigma K^TB^TQ & 0 \\ * & * & -\gamma^2 I & \sqrt{h}D^TQ & 0 & 0 \\ * & * & * & -Q & 0 & 0 \\ * & * & * & * & -Q & 0 \\ * & * & * & * & * & -I \end{bmatrix} < 0, \quad (17)$$

where

$$\begin{aligned} \Psi_{11} &= PA + A^TP + hS_{11} + S_{13} + S_{13}^T, \\ \Psi_{12} &= bPBK + hS_{12} - S_{13} + S_{23}^T, \\ \Psi_{22} &= hS_{22} - S_{23} - S_{23}^T. \end{aligned} \quad (18)$$

Proof. Considering a Lyapunov-Krasovskii functional as follows:

$$\begin{aligned} V(t) &= V_1(t) + V_2(t) = x^T(t)Px(t) \\ &\quad + \int_{-h}^{0}\int_{t+\theta}^{t} \dot{x}^T(s)Q\dot{x}(s)\,ds\,d\theta, \end{aligned} \quad (19)$$

where $P > 0$ and $Q > 0$ are matrices to be determined.

The infinitesimal operator $\mathscr{L}$ of $V(t)$ is defined as [26]

$$\mathscr{L}V(t) = \lim_{\Delta \to 0^+} \frac{1}{\Delta}\{E\{V(t+\Delta) - V(t)\}\}. \quad (20)$$

Combining (19) and (20) yields

$$\mathscr{L}V(t) = \mathscr{L}V_1(t) + \mathscr{L}V_2(t), \quad (21)$$

where

$$\begin{aligned} \mathscr{L}V_1 &= 2E\left\{x^T(t)P\dot{x}(t)\right\} \\ &= 2E\left\{x^T(t)P\left(Ax(t) + r(t)BKx(t-d(t)) + Df(t)\right)\right\} \\ &= x^T(t)\left(PA + A^TP\right)x(t) + 2x^T(t)bPBKx(t-d(t)) \\ &\quad + 2x^T(t)PDf(t). \end{aligned} \quad (22)$$

$$\begin{aligned} \mathscr{L}V_2 &= hE\left\{\dot{x}^T(t)Q\dot{x}(t)\right\} - E\left\{\int_{t-h}^{t}\dot{x}^T(s)Q\dot{x}(s)\,ds\right\} \\ &= h\Big(x^T(t)A^TQAx(t) \\ &\quad + x^T(t)\left(bA^TQBK + \left(bA^TQBK\right)^T\right)x(t-d(t)) \\ &\quad + x^T(t)A^TQDf(t) \\ &\quad + x^T(t-d(t))\alpha K^TB^TQBKx(t-d(t)) \\ &\quad + x^T(t-d(t))bK^TB^TQDf(t) \\ &\quad + f^T(t)D^TQDf(t)\Big) \\ &\quad - E\left\{\int_{t-h}^{t}\dot{x}^T(s)Q\dot{x}(s)\,ds\right\}. \end{aligned} \quad (23)$$

where $\alpha = E\{r^2(t-d(t))\} = E\{r^2(t)\} = b^2 + \sigma^2$.

From (16), we have

$$\begin{aligned} 0 &\leq E\int_{t-d(t)}^{t} \begin{bmatrix} x(t) \\ x(t-d(t)) \\ \dot{x}(s) \end{bmatrix}^T \begin{bmatrix} S_{11} & S_{12} & S_{13} \\ * & S_{22} & S_{23} \\ * & * & Q \end{bmatrix} \\ &\quad \times \begin{bmatrix} x(t) \\ x(t-d(t)) \\ \dot{x}(s) \end{bmatrix} ds \\ &= d(t)x^T(t)S_{11}x(t) + 2d(t)x^T(t)S_{12}x(t-d(t)) \\ &\quad + 2x^T(t)\ S_{13}\int_{t-d(t)}^{t}\dot{x}(s)\,ds \\ &\quad + d(t)x^T(t-d(t))S_{22}x(t-d(t)) \\ &\quad + 2x^T(t-d(t))S_{23}E\left\{\int_{t-d(t)}^{t}\dot{x}(s)\,ds\right\} \\ &\quad + E\left\{\int_{t-d(t)}^{t}\dot{x}^T(s)Q\dot{x}(s)\,ds\right\} \leq hx^T(t)S_{11}x(t) \\ &\quad + 2hx^T(t)S_{12}x(t-d(t)) \end{aligned}$$

$$
\begin{aligned}
&+2x^T(t)S_{13}(x(t)-x(t-d(t))) \\
&+hx^T(t-d(t))S_{22}x(t-d(t)) \\
&+2x^T(t-d(t))S_{23}(x(t)-x(t-d(t))) \\
&+E\left\{\int_{t-d(t)}^{t}\dot{x}^T(s)Q\dot{x}(s)\,ds\right\} \\
=\;& x^T(t)\left(hS_{11}+S_{13}+S_{13}^T\right)x(t) \\
&+2x^T(t)\left(hS_{12}-S_{13}+S_{23}^T\right)x(t-d(t)) \\
&+x^T(t-d(t))\left(hS_{22}-S_{23}-S_{23}^T\right)x(t-d(t)) \\
&+E\left\{\int_{t-d(t)}^{t}\dot{x}^T(s)Q\dot{x}(s)\,ds\right\}.
\end{aligned} \tag{24}
$$

Combining (21)–(24), one yields

$$
\begin{aligned}
&\mathscr{L}V(t)+E\left\{\xi^T(t)\xi(t)-\gamma^2 f^T(t)f(t)\right\} \\
&\le \begin{bmatrix} x(t) \\ x(t-d(t)) \\ f(t)\end{bmatrix}^T \Pi \begin{bmatrix} x(t) \\ x(t-d(t)) \\ f(t)\end{bmatrix} \\
&\quad -E\left\{\int_{t-h}^{t}\dot{x}^T(s)Q\dot{x}(s)\,ds\right\} \\
&\quad +E\left\{\int_{t-d(t)}^{t}\dot{x}^T(s)Q\dot{x}(s)\,ds\right\} \\
&=\eta^T(t)\Pi\eta(t)-E\left\{\int_{t-h}^{t-d(t)}\dot{x}^T(s)Q\dot{x}(s)\,ds\right\},
\end{aligned} \tag{25}
$$

where

$$
\begin{aligned}
\eta(t) &= \left[x^T(t)\;\; x^T(t-d(t))\;\; f^T(t)\right]^T, \\
\Pi &= \begin{bmatrix} \Phi_{11} & \Phi_{12} & PD+hA^TQD \\ * & \Phi_{22} & hbK^TB^TQD \\ * & * & hD^TRD-\gamma^2 I\end{bmatrix}, \\
\Phi_{11} &= PA+A^TP+hA^TQA+hS_{11}+S_{13}+S_{13}^T+C_1^TC_1, \\
\Phi_{12} &= bPBK+hbA^TQBK+hS_{12}-S_{13}+S_{23}^T, \\
\Phi_{22} &= h\alpha K^TB^TQBK+hS_{22}-S_{23}-S_{23}^T.
\end{aligned} \tag{26}
$$

By Lemma 2, it can be obtained from (17) that

$$
\Pi < 0. \tag{27}
$$

It follows from (25)–(27) that

$$
\mathscr{L}V(t)+E\left\{\xi^T(t)\xi(t)-\gamma^2 f^T(t)f(t)\right\}<0. \tag{28}
$$

When $f(t)=0$, it is easy to get from (28) that $\mathscr{L}V(t)<0$, which means that system (15) with $f(t)=0$ is asymptotically mean-square stable.

On the other hand, integrating both sides of (28) from 0 to ∞ and noting the fact that $V(0)=0$ under zero initial condition and $V(\infty)\ge 0$, we obtain

$$
\int_0^{\infty} E\left\{\xi^T(t)\xi(t)-\gamma^2 f^T(t)f(t)\right\}dt<0, \tag{29}
$$

which indicates that the H_∞ disturbance attenuation (11) is guaranteed.

This completes the proof. □

3.2. Sampled-Data H_∞ Controller Design. In this section, the controller design problem is solved in the following and the controller gain matrix is given in terms of a solution to LMIs.

Theorem 5. *Given scalars $h>0$, $b>0$ and $\sigma>0$, the closed-loop system* (15) *with $f(t)=0$ is asymptotically mean-square stable and the H_∞ disturbance attenuation in* (11) *is satisfied for the wave force $f(t)\in L_2[0,\infty)$ and a prescribed $\gamma>0$, if there exist matrices $X>0$, $\widehat{Q}>0$, $W>0$, $\overline{S}_{11}>0$, $\overline{S}_{12}$, $\overline{S}_{13}$, $\overline{S}_{22}>0$, and $\overline{S}_{23}$ with appropriate dimensions such that the following LMIs hold:*

$$
\begin{gathered}
\begin{bmatrix} \overline{S}_{11} & \overline{S}_{12} & \overline{S}_{13} \\ * & \overline{S}_{22} & \overline{S}_{23} \\ * & * & 2X-\widehat{Q}\end{bmatrix} \ge 0, \\
\begin{bmatrix}
\overline{\Psi}_{11} & \overline{\Psi}_{12} & D & \sqrt{h}XA^T & 0 & XC_1^T \\
* & \overline{\Psi}_{22} & 0 & \sqrt{h}bW^TB^T & \sqrt{h}\sigma W^TB^T & 0 \\
* & * & -\gamma^2 I & \sqrt{h}D^T & 0 & 0 \\
* & * & * & -\widehat{Q} & 0 & 0 \\
* & * & * & * & -\widehat{Q} & 0 \\
* & * & * & * & * & -I
\end{bmatrix} < 0,
\end{gathered} \tag{30}
$$

where

$$
\begin{aligned}
\overline{\Psi}_{11} &= AX+XA^T+h\overline{S}_{11}+\overline{S}_{13}+\overline{S}_{13}^T, \\
\overline{\Psi}_{12} &= bBW+h\overline{S}_{12}-\overline{S}_{13}+\overline{S}_{23}^T, \\
\overline{\Psi}_{22} &= h\overline{S}_{22}-\overline{S}_{23}-\overline{S}_{23}^T.
\end{aligned} \tag{31}
$$

Moreover, if inequalities (30) *have a feasible solution, then the controller gain matrix in* (8) *is given by*

$$
K=WX^{-1}. \tag{32}
$$

Proof. By pre- and postmultiplying (16) by $\operatorname{diag}\{P^{-1},P^{-1},P^{-1}\}$ and pre- and postmultiplying (17) by $\operatorname{diag}\{P^{-1},P^{-1},I,Q^{-1},Q^{-1},I\}$, (16) and (17) can be converted into the following equivalent inequalities:

$$
\begin{gathered}
\begin{bmatrix} \overline{S}_{11} & \overline{S}_{12} & \overline{S}_{13} \\ * & \overline{S}_{22} & \overline{S}_{23} \\ * & * & \overline{Q}\end{bmatrix} \ge 0, \\
\begin{bmatrix}
\overline{\Psi}_{11} & \overline{\Psi}_{12} & D & \sqrt{h}P^{-1}A^T & 0 & P^{-1}C_1^T \\
* & \overline{\Psi}_{22} & 0 & \sqrt{h}bP^{-1}K^TB^T & \sqrt{h}\sigma P^{-1}K^TB^T & 0 \\
* & * & -\gamma^2 I & \sqrt{h}D^T & 0 & 0 \\
* & * & * & -Q^{-1} & 0 & 0 \\
* & * & * & * & -Q^{-1} & 0 \\
* & * & * & * & * & -I
\end{bmatrix} < 0,
\end{gathered} \tag{33}
$$

Table 1: Parameters of the offshore platform system with an AMD mechanism.

Description	Symbol	Value	Unit
Length of the offshore platform	L	249	m
Diameter of the cylinder	$\widetilde{D}$	1.83	m
Mass of the offshore platform	m_1	7,825,307	kg
Mass of the AMD	m_2	78,253	kg
Natural frequency of the offshore platform	ω_1	2.0466	rad/s
Natural frequency of the AMD	ω_2	2.0074	rad/s
Damping ration of the offshore platform	ξ_1	0.02	—
Damping ration of the AMD	ξ_2	0.2	—

Table 2: Parameters of the wave acting on the offshore platform.

Description	Symbol	Value	Unit
Significant wave height	H_s	4	m
Water depth	d	13.2	m
Peak frequency of wave	ω_0	0.87	rad/s
Drag coefficient	C_d	1.2	—
Inertia coefficient	C_m	2.0	—
Peakedness coefficient	$\overline{\gamma}$	3.3	—
Density of water	ρ	1025.6	kg/m^3

where

$$\begin{gathered} \overline{S}_{11} = P^{-1}S_{11}P^{-1}, \qquad \overline{S}_{12} = P^{-1}S_{12}P^{-1}, \\ \overline{S}_{13} = P^{-1}S_{13}P^{-1}, \qquad \overline{S}_{22} = P^{-1}S_{22}P^{-1}, \\ \overline{S}_{23} = P^{-1}S_{23}P^{-1}, \qquad \overline{Q} = P^{-1}QP^{-1}, \\ \overline{\Psi}_{11} = AP^{-1} + P^{-1}A^T + h\overline{S}_{11} + \overline{S}_{13} + \overline{S}_{13}^T, \\ \overline{\Psi}_{12} = bBKP^{-1} + h\overline{S}_{12} - \overline{S}_{13} + \overline{S}_{23}^T, \\ \overline{\Psi}_{22} = h\overline{S}_{22} - \overline{S}_{23} - \overline{S}_{23}^T. \end{gathered} \tag{34}$$

Noting that $(Q^{-1} - P^{-1})^T Q (Q^{-1} - P^{-1}) \geq 0$, one has

$$\overline{Q} = P^{-1}QP^{-1} \geq 2P^{-1} - Q^{-1}. \tag{35}$$

By letting $X = P^{-1}$, $W = KP^{-1}$, and $\widehat{Q} = Q^{-1}$, we obtain that (33) hold if (30) is satisfied. Then, by Theorem 4, we can conclude that the theorem is true. The proof is completed. □

4. Simulation Results

In this section, the parameters of an offshore platform and the wave are given first. Then, the proposed robust sampled-data H_∞ control (RSDHC) scheme will be applied to control the offshore platform. In order to verify the feasibility and effectiveness of the proposed scheme, simulation results of the numerical example are presented. Besides, the effect of missing signal $r(t_k)$ on the H_∞ control for the offshore platform will be investigated.

4.1. The Parameters of the Offshore Platform and the External Wave Force. In Figure 1, the masses, natural frequencies, and the damping ratios of the offshore platform and the AMD and other related parameters of the offshore platform are the same as those in [11], which are listed in Table 1, where L denotes the length of the offshore platform and $\widetilde{D}$ represents the diameter of the cylinder. Based on the settings in Table 1, the matrices A, B, and D in (3) can be calculated as

$$\begin{gathered} A = \begin{bmatrix} 0 & 0 & 1.0000 & 0 \\ 0 & 0 & 0 & 1.0000 \\ -4.2290 & 0.0403 & -0.0899 & 0.0080 \\ 4.0297 & -4.0297 & 0.8030 & -0.8030 \end{bmatrix}, \\ B = 10^{-4} \times \begin{bmatrix} 0 & 0 & -0.0013 & 0.1278 \end{bmatrix}^T, \\ D = 10^{-6} \times \begin{bmatrix} 0 & 0 & 0.1278 & 0 \end{bmatrix}^T. \end{gathered} \tag{36}$$

To investigate the effectiveness of the proposed control scheme, we need to compute the values of wave force, which can be solved by referring to [6]. The parameters regarding the external wave are taken from [6] and listed in Table 2, where H_s is the significant wave height, d is the water depth, ω_0 is the peak frequency, C_d and C_m are the drag and inertia coefficients, respectively, $\overline{\gamma}$ is the peakedness coefficient, and ρ is the fluid density. Based on the settings in Table 2, the power spectrum density (PSD) of wave elevation is shown in Figure 2. The shape function $\phi(z)$ is given as [6]

$$\phi(z) = 1 - \cos\left(\frac{\pi z}{2L}\right), \qquad 0 \leq z \leq L, \tag{37}$$

where z is the vertical coordinate with the origin at the sea floor.

Then, one can compute the wave force $f(t)$ according to [6], which is shown in Figure 3.

Due to the irregular nature of the wave force adopted in this paper, we investigate both the peak values and the root mean square (RMS) values of displacement and velocity of the offshore platform and the control force [11]. The same terms M_d, M_v, and M_u are used to represent the peak values of displacement, velocity of the offshore platform, and the required control force, respectively. J_d, J_v, and J_u denote the

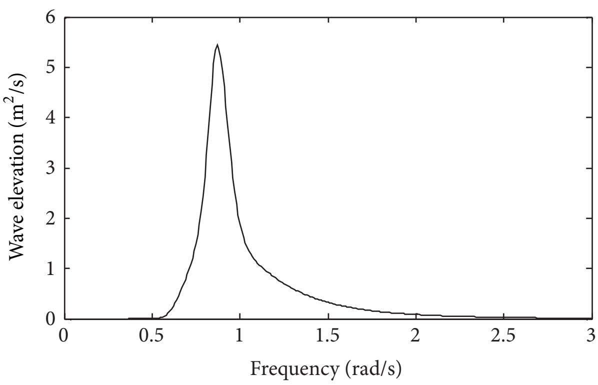

FIGURE 2: PSD of wave elevation.

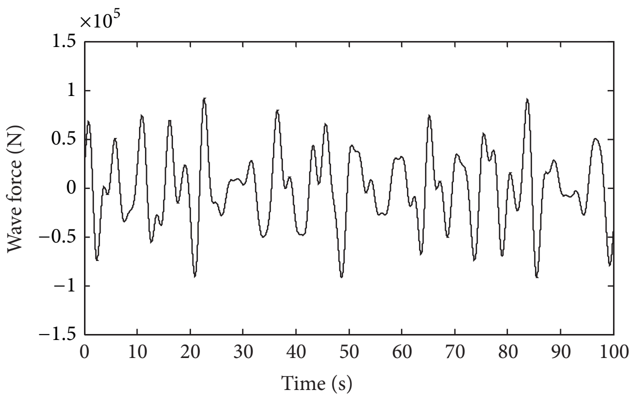

FIGURE 3: Wave force acting on the offshore structure.

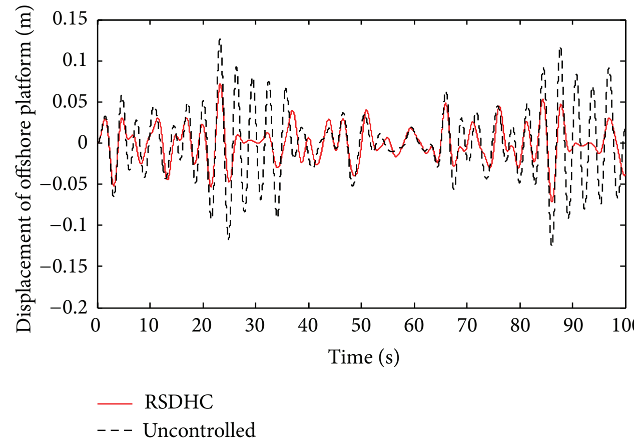

FIGURE 4: Displacement of offshore platform.

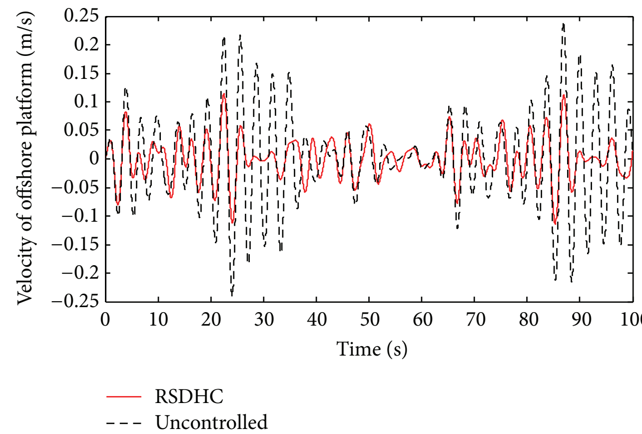

FIGURE 5: Velocity of offshore platform.

RMS values of displacement, velocity of the offshore platform, and the control force, respectively, where

$$M_d = \max\{|x_1(t)|, t \in [0, T_s]\}, \qquad J_d = \sqrt{\frac{1}{T_s}\int_0^T x_1^2(t)\,dt},$$
$$M_v = \max\{|x_3(t)|, t \in [0, T_s]\}, \qquad J_v = \sqrt{\frac{1}{T_s}\int_0^T x_3^2(t)\,dt},$$
$$M_u = \max\{|u(t)|, t \in [0, T_s]\}, \qquad J_u = \sqrt{\frac{1}{T_s}\int_0^T u^2(t)\,dt}, \tag{38}$$

with T_s as a given measurement period.

4.2. Simulation Results of RSDHC for Offshore Platform with Missing Measurements. In this section, simulation results of RSDHC for offshore platform with missing measurements are presented. Let $h = 0.02$ s, $\gamma = 0.3$ and let the probabilistic density function of $r(t_k)$ in [0, 1] be described by

$$q(r(t_k)) = \begin{cases} 0, & r(t_k) = 0, \\ 0.1, & r(t_k) = 0.5, \\ 0.9, & r(t_k) = 1, \end{cases} \tag{39}$$

from which the expectation and the standard deviation can be easily calculated as $b = 0.95$ and $\sigma = 0.15$. Then, by Theorem 5, the controller gain matrix K in (8) can be obtained as

$$K = 10^5 \times [7.9703 \quad 0.0595 \quad 1.1646 \quad -0.0747]. \tag{40}$$

We give the displacement, velocity, and acceleration curves of the offshore platform system without control and with RSDHC in Figures 4, 5, and 6, respectively. The corresponding control curves are presented in Figure 7. When the RSDHC is used to control the offshore platform, the peak values of displacement and velocity of the offshore platform are reduced from 0.1264 m and 0.2419 m/s to 0.0719 m and 0.1149 m/s, respectively. The maximum control force required is about 3.7397×10^4 N. The RMS values of displacement and the velocity are reduced from 0.0424 m and 0.0826 m/s to 0.0223 m and 0.0365 m/s, respectively, and the RMS value of control force is about 1.4539×10^4 N.

The peak and RMS values of displacement, velocity of the offshore platform under no control and RSDHC, and the corresponding control force for different values of γ are listed in Table 3, where $b = 0.95$ and $\sigma = 0.15$. Based on

Table 3: The peak and RMS values of displacement and velocity for different values of γ.

	Peak value			RMS value		
	M_d (m)	M_v (m/s)	M_u (10^4 N)	J_d (m)	J_v (m/s)	J_u (10^4 N)
No control	0.1264	0.2419		0.0424	0.0826	
$\gamma = 0.2$	0.0699	0.1114	3.9404	0.0220	0.0355	1.5610
$\gamma = 0.3$	0.0719	0.1149	3.7397	0.0223	0.0365	1.4539
$\gamma = 0.9$	0.0720	0.1150	4.6481	0.0223	0.0365	1.7257

Table 4: The average peak and RMS values reduction of displacement and velocity.

Controller	Reduction of peak value		Reduction of RMS value	
	Displacement (%)	Velocity (%)	Displacement (%)	Velocity (%)
RSDHC	43.62	52.97	47.64	56.21

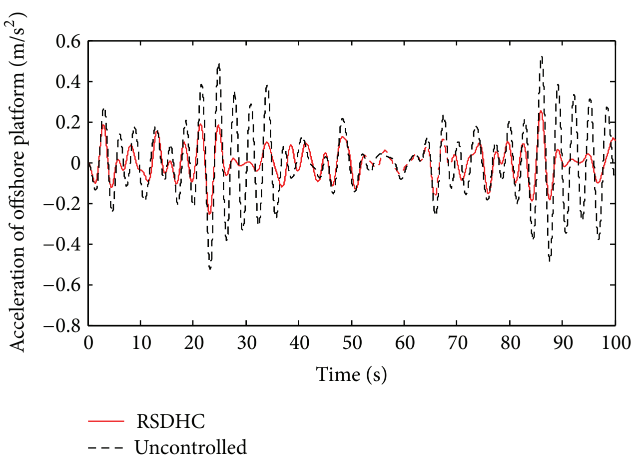

Figure 6: Acceleration of offshore platform.

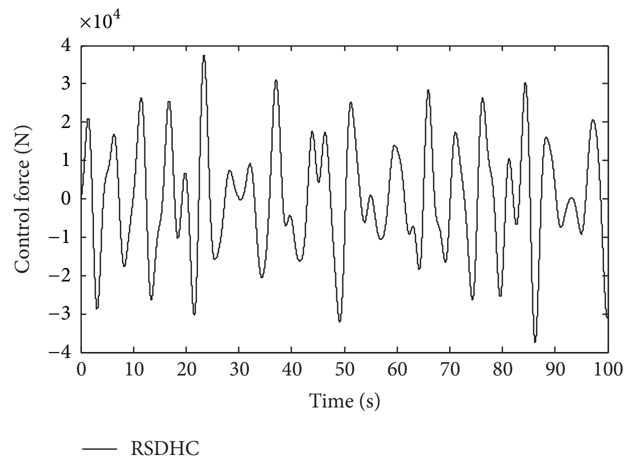

Figure 7: Control force of offshore platform.

Table 3, one can yield the average reduction of peak and RMS values of the offshore platform under RSDHC with missing measurements, which are presented in Table 4.

From Figures 4–6 and Tables 3-4, it can be found that the proposed RSDHC scheme is effective. The peak and RMS values of the displacement are reduced by about 43 percent and 47 percent of the ones without control, respectively, and the peak and RMS values of the velocity are reduced by 52 percent and 56 percent of the ones without control, respectively. From Figure 6, we can see that the acceleration of offshore platform has been decreased significantly.

4.3. Effects of the Missing Signal $r(t_k)$ on RSDHC for Offshore Platform. Now, we turn to investigate the effects of the artificially introduced missing signal $r(t_k)$ on robust sampled-data H_∞ control for offshore structure. First, we give four missing signals with different probabilistic density functions, and their expectations and standard deviations are computed, which are listed in Table 5. For the cases of the different introduced missing signals, the peak and RMS values of displacement, velocity of the offshore platform, and the control force are computed and listed in Table 6, where $\gamma = 0.3$. Based on Table 6, one can yield the reduction of peak and RMS values of the offshore platform under RSDHC, which are presented in Table 7.

From Tables 6 and 7, it can be seen that the proposed RSDHC scheme is effective to control the offshore platform, even though the expectation and standard deviation of the missing signal are 0.25 and 0.34, respectively. In addition, we can find that the peak and RMS values reduction of displacement and velocity become smaller with the decrease of b and σ.

5. Conclusions

In this paper, we have developed the problem of vibration control for offshore platforms with missing measurements subject to external wave. A robust sampled-data H_∞ control scheme has been proposed. It is found from the simulation results that the designed scheme is effective to attenuate the external wave force and thereby improve the control performance of the offshore platform. In our further work,

Table 5: Probabilistic density functions, expectations, and standard deviations of missing signal $r(t_k)$.

	Probabilistic density function			Expectation	Standard deviation
$q_1(r_1(t_k))$	0	0.1	0.9	0.95	0.15
$r_1(t_k)$	0	0.5	1		
$q_2(r_2(t_k))$	0.2	0.2	0.6	0.7	0.4
$r_2(t_k)$	0	0.5	1		
$q_3(r_3(t_k))$	0.3	0.5	0.2	0.45	0.35
$r_3(t_k)$	0	0.5	1		
$q_4(r_4(t_k))$	0.6	0.3	0.1	0.25	0.34
$r_4(t_k)$	0	0.5	1		

Table 6: The peak and RMS values of displacement and velocity for different missing signals $r(t_k)$.

	Peak value			RMS value		
	M_d (m)	M_v (m/s)	M_u (10^4 N)	J_d (m)	J_v (m/s)	J_u (10^4 N)
No control	0.1264	0.2419		0.0424	0.0826	
No missing	0.0690	0.1100	3.7989	0.0218	0.0351	1.5415
$b = 0.95, \sigma = 0.15$	0.0719	0.1149	3.7397	0.0223	0.0365	1.4539
$b = 0.70, \sigma = 0.40$	0.0746	0.1191	5.7289	0.0229	0.0377	2.0809
$b = 0.45, \sigma = 0.35$	0.0821	0.1370	11.570	0.0246	0.0420	3.7421
$b = 0.25, \sigma = 0.34$	0.0981	0.1760	5.8798	0.0290	0.0530	1.7157

Table 7: The peak and RMS values reduction of displacement and velocity.

	Reduction of peak value		Reduction of RMS value	
	Displacement (%)	Velocity (%)	Displacement (%)	Velocity (%)
No missing	45.41	54.53	48.58	57.51
$b = 0.95, \sigma = 0.15$	43.12	52.50	47.41	55.81
$b = 0.70, \sigma = 0.40$	40.98	50.76	45.99	54.36
$b = 0.45, \sigma = 0.35$	35.05	43.37	41.98	49.15
$b = 0.25, \sigma = 0.34$	22.39	27.24	31.60	35.84

we will extend the proposed results to the case of multiple missing measurements of sensors. Also, we can investigate the sampled-data H_2/H_∞ control for vibration attenuation of offshore platforms subject to multiple external forces. In addition, we may consider the sampled-data H_∞ control for offshore platforms by using the finite frequency approach [30, 31].

Conflict of Interests

The authors declare that there is no conflict of interests regarding the publication of this paper.

Acknowledgments

This work has been supported by the National Natural Science Foundation of China under Grant no. 61273120 and by Norwegian Centre for Offshore Wind Energy (NORCOWE) under Grant no. 193821/S60 from Research Council of Norway (RCN). NORCOWE is a consortium with partners from industry and science, hosted by Christian Michelsen Research.

References

[1] M. J. Terro, M. S. Mahmoud, and M. Abdel-Rohman, "Multi-loop feedback control of offshore steel jacket platforms," *Computers & Structures*, vol. 70, no. 2, pp. 185–202, 1999.

[2] M. Zribi, N. Almutairi, M. Abdel-Rohman, and M. Terro, "Nonlinear and robust control schemes for offshore steel jacket platforms," *Nonlinear Dynamics*, vol. 35, no. 1, pp. 61–80, 2004.

[3] H. J. Li, S.-L. J. Hu, and C. Jakubiak, "H_2 active vibration control for offshore platform subjected to wave loading," *Journal of Sound and Vibration*, vol. 263, no. 4, pp. 709–724, 2003.

[4] H. Ma, G.-Y. Tang, and Y.-D. Zhao, "Feedforward and feedback optimal control for offshore structures subjected to irregular wave forces," *Ocean Engineering*, vol. 33, no. 8-9, pp. 1105–1117, 2006.

[5] M. Luo and W. Q. Zhu, "Nonlinear stochastic optimal control of offshore platforms under wave loading," *Journal of Sound and Vibration*, vol. 296, no. 4-5, pp. 734–745, 2006.

[6] H. Ma, G.-Y. Tang, and W. Hu, "Feedforward and feedback optimal control with memory for offshore platforms under irregular wave forces," *Journal of Sound and Vibration*, vol. 328, no. 4-5, pp. 369–381, 2009.

[7] X.-M. Zhang, Q.-L. Han, and D. Han, "Effects of small time-delays on dynamic output feedback control of offshore steel

jacket structures," *Journal of Sound and Vibration*, vol. 330, no. 16, pp. 3883–3900, 2011.

[8] B.-L. Zhang, Q.-L. Han, X.-M. Zhang, and X. Yu, "Integral sliding mode control for offshore steel jacket platforms," *Journal of Sound and Vibration*, vol. 331, no. 14, pp. 3271–3285, 2012.

[9] B.-L. Zhang, L. Ma, and Q.-L. Han, "Sliding mode H_∞ control for offshore steel jacket platforms subject to nonlinear self-excited wave force and external disturbance," *Nonlinear Analysis: Real World Applications*, vol. 14, no. 1, pp. 163–178, 2013.

[10] B.-L. Zhang, Y.-H. Hu, and G.-Y. Tang, "Stabilization control for offshore steel jacket platforms with actuator time-delays," *Nonlinear Dynamics*, vol. 70, no. 2, pp. 1593–1603, 2012.

[11] B. L. Zhang and G. Y. Tang, "Active vibration H_∞ control of offshore steel jacket platforms using delayed feedback," *Journal of Sound and Vibration*, vol. 332, no. 22, pp. 5662–5677, 2013.

[12] T. Chen and B. Francis, *Optimal Sampled-Data Control Systems*, Springer, London, UK, 1995.

[13] Z. Li, Y. Yu, D. Jiao, J. Wang, Z. Li, and J. Ou, "Development of fast wireless detection system for fixed offshore platform," in *Sensors and Smart Structures Technologies for Civil, Mechanical, and Aerospace Systems*, vol. 7981 of *Proceedings of SPIE*, p. 8, San Diego, Calif, USA, March 2011, 79811N.

[14] W. Hong, Z. Zhou, and J. Ou, "Offshore platform health monitoring applications of wireless sensor network," in *Proceedings of the 21st International Modal Analysis Conference*, Orlando, Fla, USA, 2003.

[15] Y. Yu and J. Ou, "Wireless sensing experiments for structural vibration monitoring of offshore platform," *Frontiers of Electrical and Electronic Engineering in China*, vol. 3, no. 3, pp. 333–337, 2008.

[16] S. Petersen and S. Carlsen, "Wireless sensor networks: introduction to installation and integration on an offshore oil & gas platform," in *Proceedings of the 19th Australian Conference on Software Engineering (ASWEC '08)*, p. 53, Perth, Australia, March 2008.

[17] J. P. Lynch and K. J. Loh, "A summary review of wireless sensors and sensor networks for structural health monitoring," *Shock and Vibration Digest*, vol. 38, no. 2, pp. 91–130, 2006.

[18] J. Lei, "Delayed semiactive control of offshore platform in high-speed communication networks," in *Proceedings of the International Conference on System Science and Engineering (ICSSE '11)*, pp. 199–204, Macau, China, June 2011.

[19] J. P. Hespanha, P. Naghshtabrizi, and Y. Xu, "A survey of recent results in networked control systems," *Proceedings of the IEEE*, vol. 95, no. 1, pp. 138–162, 2007.

[20] Z. Wang, F. Yang, D. W. C. Ho, and X. Liu, "Robust H_∞ filtering for stochastic time-delay systems with missing measurements," *IEEE Transactions on Signal Processing*, vol. 54, no. 7, pp. 2579–2587, 2006.

[21] F. Yang, Z. Wang, D. W. C. Ho, and M. Gani, "Robust H_∞ control with missing measurements and time delays," *IEEE Transactions on Automatic Control*, vol. 52, no. 9, pp. 1666–1672, 2007.

[22] H. Gao, T. Chen, and L. Wang, "Robust fault detection with missing measurements," *International Journal of Control*, vol. 81, no. 5, pp. 804–819, 2008.

[23] Z. Wang, D. W. C. Ho, Y. Liu, and X. Liu, "Robust H_∞ control for a class of nonlinear discrete time-delay stochastic systems with missing measurements," *Automatica*, vol. 45, no. 3, pp. 684–691, 2009.

[24] H. Dong, Z. Wang, D. W. C. Ho, and H. Gao, "Robust H_∞ fuzzy output-feedback control with multiple probabilistic delays and multiple missing measurements," *IEEE Transactions on Fuzzy Systems*, vol. 18, no. 4, pp. 712–725, 2010.

[25] Z. Wang, B. Shen, H. Shu, and G. Wei, "Quantized H_∞ control for nonlinear stochastic time-delay systems with missing measurements," *IEEE Transactions on Automatic Control*, vol. 57, no. 6, pp. 1431–1444, 2012.

[26] S. Xiao, W. Cheng, H. Zeng, and L. Kong, "Further results on stability of networked control systems with randomly varying delay and missing measurements," in *Proceedings of the 3rd International Conference on Intelligent System Design and Engineering Applications (ISDEA '13)*, pp. 787–790, Hong Kong, January 2013.

[27] E. Fridman, A. Seuret, and J.-P. Richard, "Robust sampled-data stabilization of linear systems: an input delay approach," *Automatica*, vol. 40, no. 8, pp. 1441–1446, 2004.

[28] E. Fridman, U. Shaked, and V. Suplin, "Input/output delay approach to robust sampled-data H_∞ control," *Systems & Control Letters*, vol. 54, no. 3, pp. 271–282, 2005.

[29] E. Fridman, "A refined input delay approach to sampled-data control," *Automatica*, vol. 46, no. 2, pp. 421–427, 2010.

[30] W. Sun, H. Gao Sr., and O. Kaynak, "Finite frequency H_∞ control for vehicle active suspension systems," *IEEE Transactions on Control Systems Technology*, vol. 19, no. 2, pp. 416–422, 2011.

[31] W. Sun, Y. Zhao, J. Li, L. Zhang, and H. Gao, "Active suspension control with frequency band constraints and actuator input delay," *IEEE Transactions on Industrial Electronics*, vol. 59, no. 1, pp. 530–537, 2012.

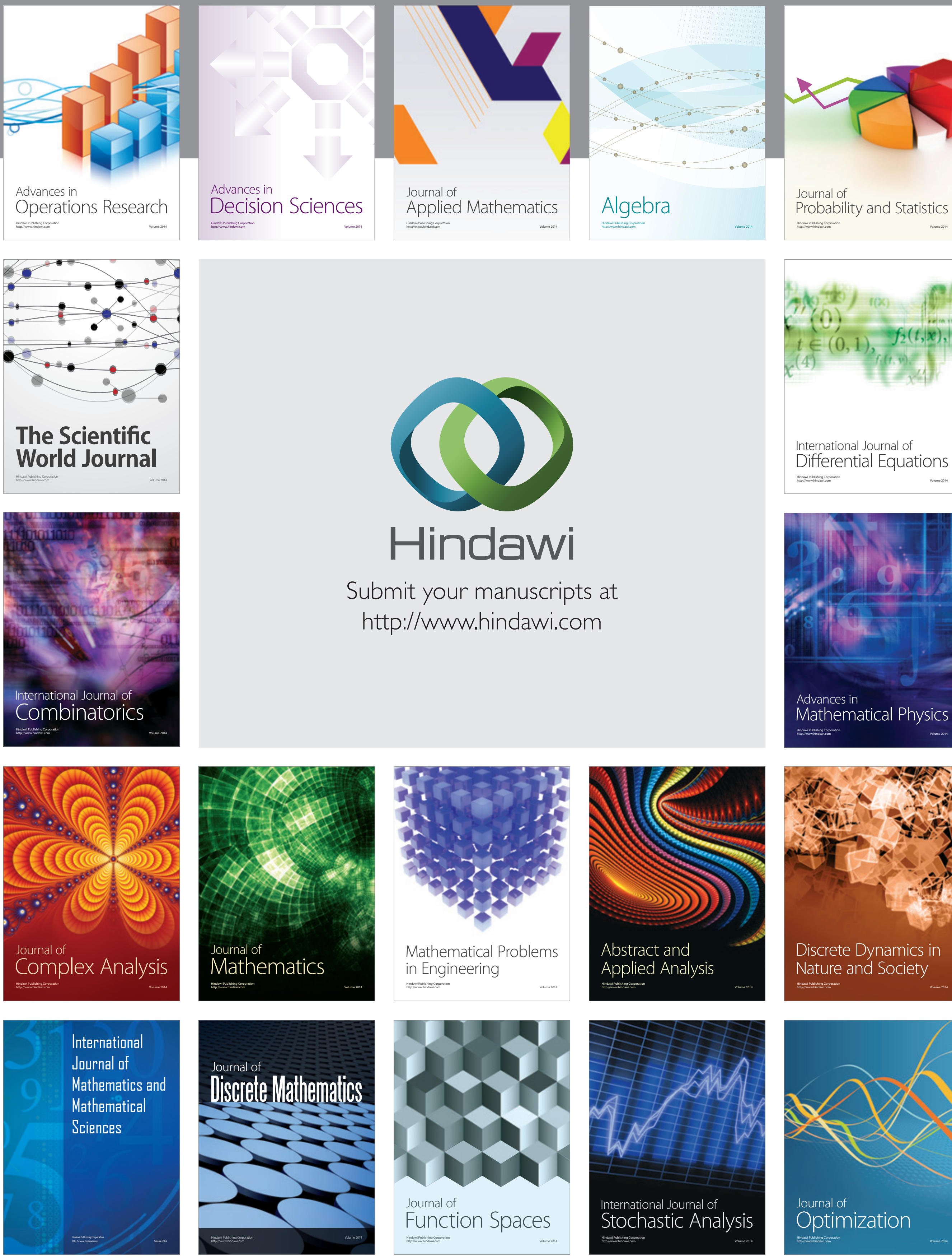
Advances in Operations Research
Advances in Decision Sciences
Journal of Applied Mathematics
Algebra
Journal of Probability and Statistics
The Scientific World Journal
Hindawi
Submit your manuscripts at
http://www.hindawi.com
International Journal of Differential Equations
International Journal of Combinatorics
Advances in Mathematical Physics
Journal of Complex Analysis
Journal of Mathematics
Mathematical Problems in Engineering
Abstract and Applied Analysis
Discrete Dynamics in Nature and Society
International Journal of Mathematics and Mathematical Sciences
Journal of Discrete Mathematics
Journal of Function Spaces
International Journal of Stochastic Analysis
Journal of Optimization